



OPE

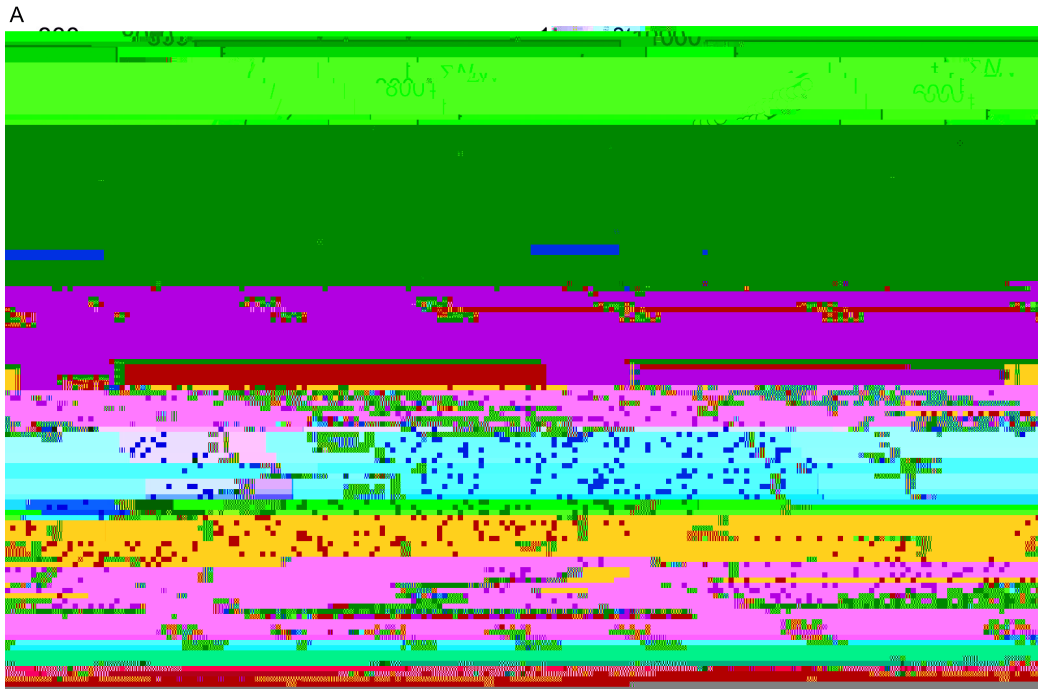


FIGURE 2 | The andesitic-dacitic volcano Soufriere Hills, Montserrat, erupted on 15 November 1995 after 350 years of repose. VT data from three sources are consistent with initial and final episodes of accelerating VT event rate separated by an interval of constant event rate. **(A)** 01 January–31 July (time t



FIGURE 3 | The number of VT events may accelerate with time (top), while the mean deformation rate remains constant (bottom, gradient of broken line). The example shows VT and deformation trends before the flank eruption of Mauna Ulu on Kilauea, Hawaii, on 04 February 1972 (most VT events had magnitudes between 1.5 and 4; Bell and Kilburn, 2011). In this case, the VT number, δN , increases exponentially with time t (in days; broken curve) as $1.17 \exp(t/23.3)$; the mean daily VT event rate increases $0.05 \exp(t/23.3)$. The combination of exponential VT rate and constant deformation rate is consistent with quasi-elastic brittle behavior under a constant rate of stress supply (**Table 1**). The eruption occurred almost immediately after the end of the quasi-elastic regime when $t/23.3 \approx 4$.

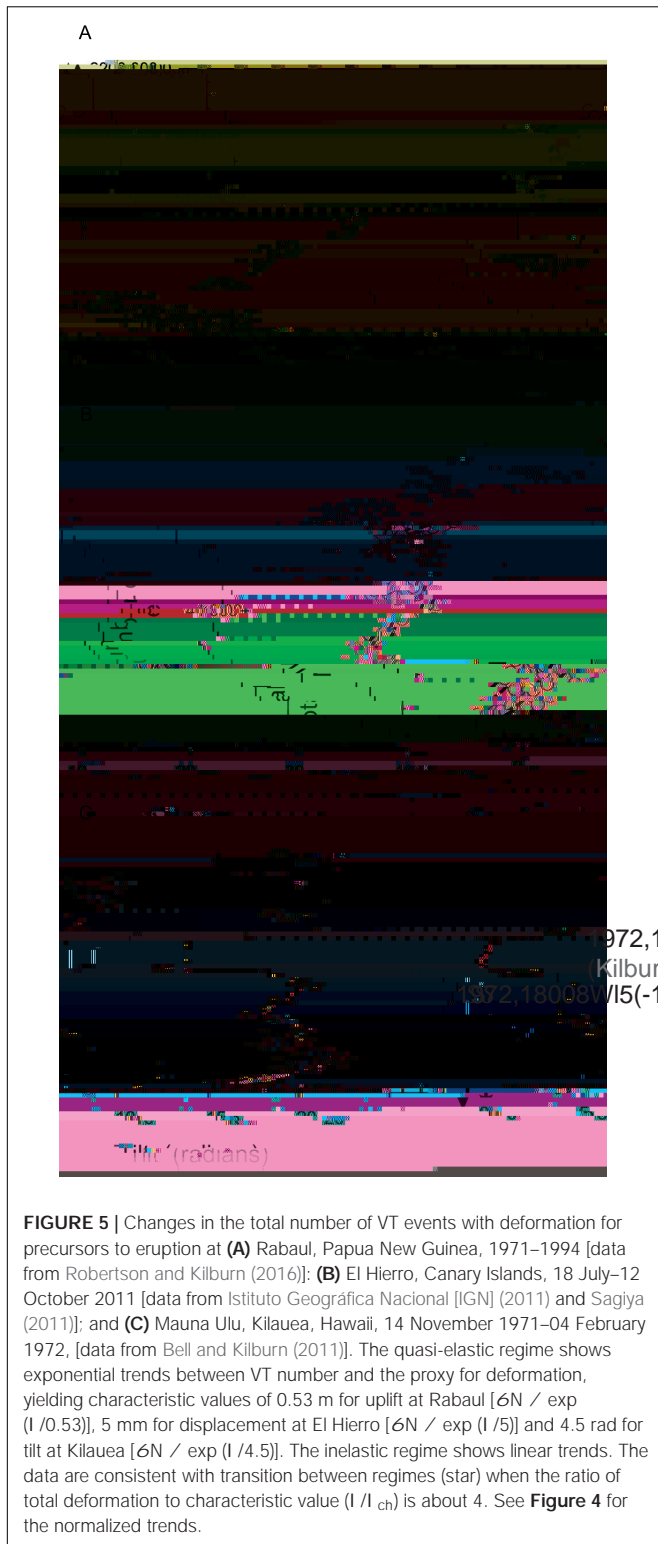


FIGURE 5 | Changes in the total number of VT events with deformation for precursors to eruption at **(A)** Rabaul, Papua New Guinea, 1971–1994 [data from Robertson and Kilburn (2016)]; **(B)** El Hierro, Canary Islands, 18 July–12 October 2011 [data from Instituto Geográfica Nacional [IGN] (2011) and Sagiya (2011)]; and **(C)** Mauna Ulu, Kilauea, Hawaii, 14 November 1971–04 February 1972, [data from Bell and Kilburn (2011)]. The quasi-elastic regime shows exponential trends between VT number and the proxy for deformation, yielding characteristic values of 0.53 m for uplift at Rabaul [$\delta N / \exp(I / 0.53)$], 5 mm for displacement at El Hierro [$\delta N / \exp(I / 5)$] and 4.5 rad for tilt at Kilauea [$\delta N / \exp(I / 4.5)$]. The inelastic regime shows linear trends. The data are consistent with transition between regimes (star) when the ratio of total deformation to characteristic value (I / I_{ch}) is about 4. See **Figure 4** for the normalized trends.

body and, as demonstrated below, the precursory sequences at Pinatubo and Soufriere Hills can be explained more simply by equating S_{ch} instead with the tensile strength.

APPLICATIONS TO FIELD DATA

Changes in Seismicity With Deformation

Equations (4 and 5) describe the change from an exponential to linear increase in VT number with deformation, corresponding to the evolution from quasi-elastic to inelastic behavior. In the quasi-elastic regime, $S_{supp} = S$ [Eq. (2)] and both S_{sup} and S can be set to $E\epsilon$, the product of Young's modulus and bulk deformation. If ground movement, I , is proportional to the bulk deformation, Eq. (4) yields exponential increases with ground movement of both the change in VT seismicity and the total number of VT events [Table 1, Eqs (T1) and (T2)]. In the inelastic regime, the additional elastic strain supplied by S_{sup} is consumed in faulting (Section 3). Changes in N and I now both measure VT events, so dN/dI is constant and total VT number increases linearly with ground movement [Figures 4, 5 and Table 1, and Eq. (T3)].

The transition from quasi-elastic to inelastic behavior occurs when the applied differential stress reaches its failure value, S_F . Since $S_{ch} = S_T$ for tensile deformation, the transitional value for S/S_{ch} in Eq. (4) is expected to be S_F/S_T for crust being stretched. Applying the Mohr–Coulomb–Griffith criterion for bulk failure,

$$\frac{S}{S_T} = \frac{1}{2} \left(\frac{S_F}{S_T} + \frac{S_F}{S_T} \right) \left(\frac{I}{I_{ch}} \right) \quad (47)$$

$$\frac{S}{S_T} = \frac{1}{2} \left(\frac{S_F}{S_T} + \frac{S_F}{S_T} \right) \left(\frac{I}{I_{ch}} \right) \quad (47)$$

Philippines, and 1995 eruption of Soufriere Hills, on Montserrat (Kilburn, 2003), implying the unlikely scenario of eruptions through crust in compression. Extensional stresses are instead anticipated in crust being deformed by a pressurizing magma

from the VT-deformation trends (**Figures 4, 5**), so reinforcing the interpretation of deformation in tension (**Figure 6**).

The particular value of S_F/S_T in tension changes with the geometry of failure. The generic Mohr–Coulomb–Griffith criterion applies to failure along a plane (e.g., creating a new failure plane or pulling opening a sealed fault) and values for S_F/S_T are ≤ 4 . Pressurized bodies, in contrast, rupture their margins at values of S_F/S_T that change according to their shape; for example, S_F/S_T is three for a sphere, but two for a long vertical cylinder (Jaeger, 1969; Saada, 2009). The preferred field values of 2–4 are thus consistent with the onset of bulk failure at the margins of magma bodies, as well as the opening of healed faults in crust being stretched by those bodies. In all cases, tensile bulk failure requires the effective principal stresses (normal stress – pore-fluid pressure) to be less than three times the tensile strength (**Figure 6**). For a notional strength of 10 MPa, therefore, the effective principal stress cannot exceed about 30 MPa, which corresponds to maximum lithostatic depths of about 1.2 and 2 km in dry and water-saturated crust. Tensile failure at greater depths thus implies deformation of super-saturated crust with pore-fluid pressures greater than hydrostatic (Shaw, 1980).

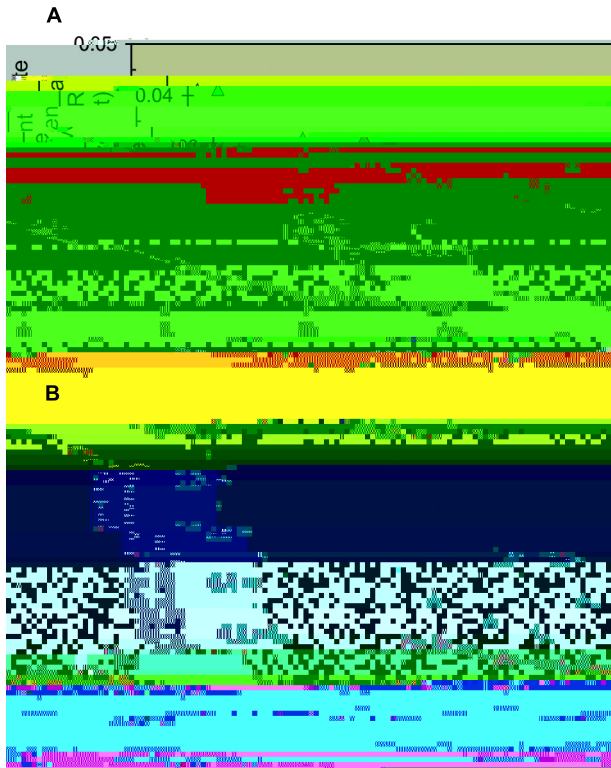


FIGURE 7 | Linear decreases (dashed lines) in inverse-rate minima for VT events (large triangles) before magmatic eruptions (arrows) after centuries of repose at **(A)** Soufriere Hills, Montserrat (gradient -2.4×10^{-7})

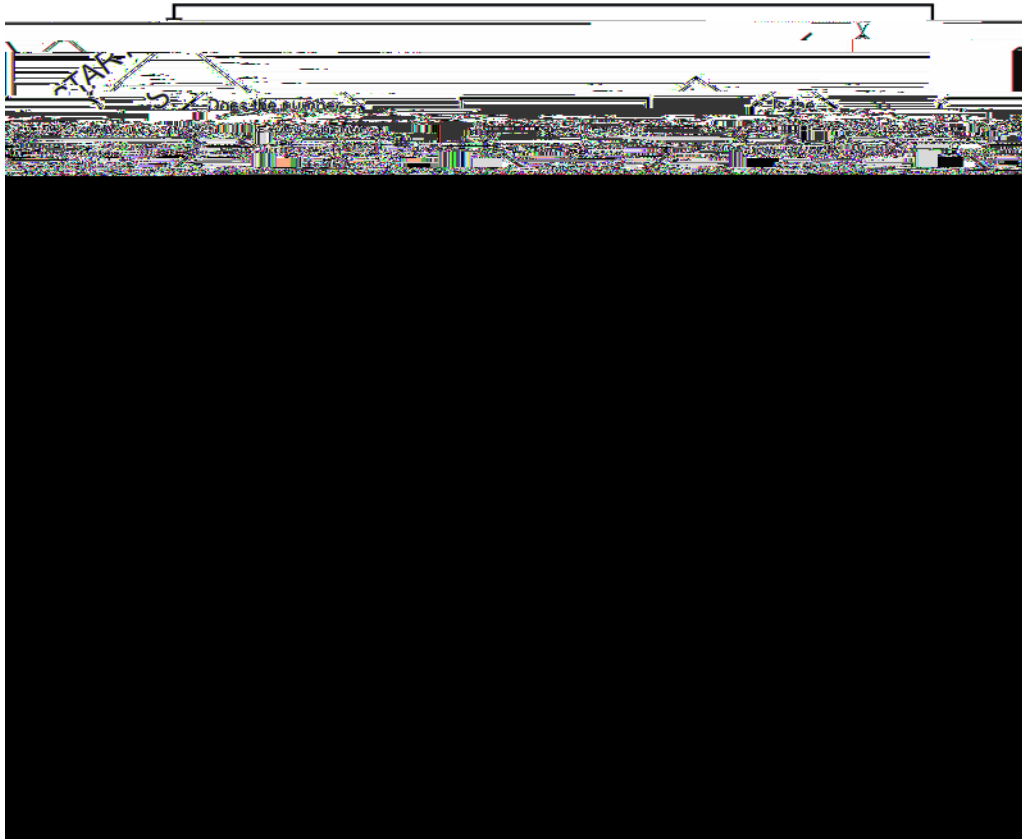


FIGURE 9 | Flow-chart showing an example the proposed operational procedure for applying the elastic-brittle model to VT and deformation signals of unrest. It assumes a transition from exponential to hyperbolic VT event rates after an amount of ground movement $4h_{ch}$ and, for a constant rate of stress supply, after a time $4t_{ch}$.

REFERENCES

- Acocella, V., Di Lorenzo, R., Newhall, C., and Scandone, R. (2015). An overview of recent (1988-2014) caldera unrest: knowledge and perspectives. *Rev. Geophys.* 53, 896–955. doi: 10.1002/2015RG000492
- Amitrano, D., Grasso, J. R., and Senfaute, G. (2005). Seismic precursory patterns before a cli collapse and critical point phenomena. *Geophys. Res. Lett.* 32:L08314. doi: 10.1029/2004GL022270
- Anderson, O. L., and Grew, P. C. (1977). Stress corrosion theory of crack propagation with applications to geophysics. *Rev. Geophys. Space Sci.* 15, 77–104. doi: 10.1029/RG015i001p00077
- Aspinall, W. (2006). "Structured elicitation of expert judgement for probabilistic hazard and risk assessment in volcanic eruptions," in *Statistics in Volcanology*, eds H. M. Mader, S. G. Coles, C. B. Connor, and L. J. Connor (Rome: IAVCEI Publications), 15–30.
- Atkinson, B. K. (1984). Subcritical crack growth in geological materials. *J. Geophys. Res.* 89, 4077–4114. doi: 10.1029/JB089iB06p04077
- Bell, A., and Kilburn, C. R. J. (2011). Precursors to dyke-fed eruptions at basaltic volcanoes: insights from the spatiotemporal patterns of volcano-tectonic seismicity at Kilauea volcano, Hawaii. *Bull. Volcanol.* 74, 325–339. doi: 10.1007/s00445-011-0519-3

- Main, I. G. (1999). Applicability of time-to-failure analysis to accelerated strain before earthquakes and volcanic eruptions. *Geophys. J. Int.* 139, F1–F6. doi: 10.1046/j.1365-246x.1999.00004.x
- Main, I. G. (2000). A damage mechanics model for power-law creep and earthquake aftershock and foreshock sequences. *Geophys. J. Int.* 142, 151–161. doi: 10.1046/j.1365-246x.2000.00136.x
- Main, I. G., and Meredith, P. G. (1991). Stress corrosion constitutive laws as a possible mechanism of intermediate-term and short-term seismic event rates and b-values. *Geophys. J. Int.* 107, 363–372. doi: 10.1111/j.1365-246X.1991.tb00831.x
- Marzocchi, W., and Bebbington, M. S. (2012). Probabilistic eruption forecasting at short and long time scales. *Bull. Volcanol.* 74:805. doi: 10.1007/s00445-012-0633-x
- McGuire, W. J., and Kilburn, C. R. J. (1997). Forecasting volcanic events: some contemporary issues. *Geol. Rundsch.* 86, 439–445. doi: 10.1007/s005310050152
- McKee, C. O., Lowenstein, P. L., De Saint Ours, P., Talai, B., Itikari, I., and Mori, J. J. (1984). Seismic and ground deformation crises at Rabaul caldera: prelude to an eruption? *Bull. Volcanol.* 47, 397–411. doi: 10.1007/BF01961569
- McNutt, S. R. (2005). Volcano seismology.